ISSN: 1692-7257 - Volume 1 – Number 47 - 2026

RCTA
Revista Colombiana de Tecnologías de Avanzada
UNIPAMPLONA

Digital Object Identifier: 10.24054/rcta.v1i47.4355

Synthesis of nickel plates coated by electrodeposition with Ni_xS_y

Síntesis de placas de níquel recubiertas mediante electrodeposición con Ni_xS_y

Físico Esteban Quintero Moreno[1,2], MSc. Héctor Darío Sánchez Londoño[1], PhD. Edwin García Quintero[1]

[1] ***Universidad de Antioquia***, *Facultad de ingeniería, Grupo de investigación TESLA, Medellín, Antioquia, Colombia.*
[2] ***ITM, Institución Universitaria***, *Facultad de Ciencias Exactas y Aplicadas, Departamento de Ciencias Básicas, Medellín, Antioquia, Colombia.*

Correspondence: *esteban.quintero@udea.edu.co*

Received: *November 12, 2025.* ***Accepted:*** *December 18, 2025.* ***Published:*** *February 09, 2026.*

How to cite: *E. Quintero Moreno, H. D. Sánchez Londoño, and E. García Quintero, "Synthesis of nickel plates coated by electrodeposition with Ni_xS_y", RCTA, vol. 1, n.º. 47, pp. 202-208, feb. 2026.*
Recovered from https://ojs.unipamplona.edu.co/index.php/rcta/article/view/4355

Abstract: The present article aims to analyze the current, voltage, and time parameters involved in the electrodeposition of nickel sulfide nanolayers on pure nickel plates through a synthesis route based on variations in the number of cycles (1, 3, 4, and 7). Each cycle consists of four different voltage steps within the range of 0.54–2.4 V, which are repeated according to the corresponding number of cycles. A nickel nitrate hexahydrate solution (0.05 mol/L) and sodium thiosulfate pentahydrate (0.1 mol/L) were used as the electrolyte. The voltage values exhibit high stability, with oscillations of ±0.2 V, indicating that the employed methods provide a high degree of control over the electrodeposition process. Additionally, a mass gain in the range of 0.44–6.57 mg was obtained for the electrodepositions.

Keywords: nanotechnology, electrodeposition, layer engineering, sulfur, nickel.

Resumen: El presente artículo tiene como objetivo analizar los parámetros de corriente, voltaje y tiempo en la electrodeposición de nanocapas de sulfuro de níquel sobre placas de níquel puro mediante una vía de síntesis basada en variaciones del número de ciclos (1, 3, 4 y 7). Cada ciclo consta de cuatro escalones de voltaje diferentes en el rango de (0.54–2.4) V, los cuales se repiten de acuerdo con el número de ciclos correspondiente. Como electrolito se utilizó una solución de nitrato de níquel hexahidratado (0.05 mol/L) y tiosulfato de sodio pentahidratado (0.1 mol/L). Los valores de voltaje presentan una alta estabilidad, con oscilaciones de ±0.2 V, lo que indica que los métodos empleados permiten un elevado control sobre el proceso de electrodeposición. Adicionalmente, se obtuvo una ganancia de masa en el rango de (0.44–6.57) mg para las electrodeposiciones realizadas.

Palabras clave: nanotecnología, electrodeposición, ingeniería de capas, azufre, níquel.

1. INTRODUCTION

The planet faces constant challenges. A few years ago, in 2023, we had already exceeded six of the planetary boundaries [1], and the following year (2025) we exceeded seven of the nine planetary boundaries [2]. One worrying element is ocean acidification, as it puts the planet's marine life at risk. Many efforts are being made to address this, including finding alternative, planet-friendly ways to produce energy. In this regard, hydrogen production [3] through water electrolysis is a valuable tool [4], [5], [6], [7]. For this, we need to delve deeper into the role of the electrodes used in the process [8] and how certain electrode doping techniques help improve the process [9], [10], [11]. Additionally, we found that electrodepositing Ni_xS_y on nickel plates is a very promising process [12], [13], for which we carried out the experimental design and characterized the deposited mass.

2. METHODOLOGY

2.1 Experimental design and factorial designs

The design and analysis of experiments allowed us to determine two central elements in the research, the first is that it allowed us to determine the determining variables of the synthesis and that have an impact on the layer thickness of the final sample and the second allowed us to determine the number of samples needed and with this, optimize the total time of the experimental phase [14], [15].

For the investigation, we constructed a two-factor factorial design for synthesis I, the number of cycles and the voltage change ($\Delta V = V_{final} - V_{initial}$). One cycle has a time of 4 min and consists of establishing a different voltage value every minute. We made the decision to construct a 4x3 factorial (4 levels for cycles and 3 levels of ΔV) with one replicate and for two differentiated treatments, which will henceforth be identified as “Synthesis I, Treatment I” and “Treatment II”, which can be observed in the following figures respectively, Figure 1 and Figure 2. Additionally, we present the tables, Table 1 and Table 2 with the respective values.

It is important to clarify that in the synthesis process the electrolyte has multiple factors such as concentration, temperature, agitation, among many others [16], therefore, the decision was made to keep all these factors invariant for the entire experimental phase, we do this by carrying out the same synthesis protocol without varying the electrolyte precursors, additionally the configuration of the electrodeposition system is kept invariant.

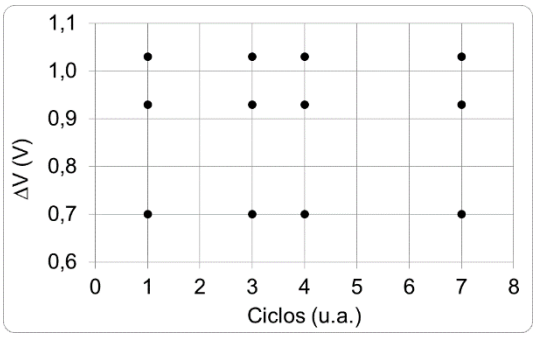

Fig. 1. *Representation of the 4 x 3 factorial design, Synthesis I, Treatment I.*

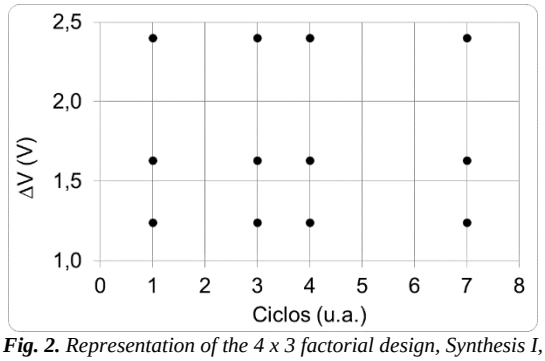

Fig. 2. *Representation of the 4 x 3 factorial design, Synthesis I, Treatment II.*

Table 1: *Data from the representation of the 4 x 3 factorial design, Synthesis I, Treatment I.*

Cycles (u.a)	ΔV (V)
1	0.70 – 0.93 – 1.03
3	0.70 – 0.93 – 1.03
4	0.70 – 0.93 – 1.03
7	0.70 – 0.93 – 1.03

Table 2: *Data from the representation of the 4 x 3 factorial design, Synthesis I, Treatment II.*

Cycles (u.a)	ΔV (V)
1	1.24 – 1.63 – 2.40
3	1.24 – 1.63 – 2.40
4	1.24 – 1.63 – 2.40
7	1.24 – 1.63 – 2.40

During the synthesis process, it was decided to keep all these factors invariant throughout the entire experimental phase, which consists of 24 experiments, each with one replicate. The electrodeposition system configuration shown in Figure 4 also remains unchanged.

The nickel electrode is a square sheet with an approximate area of 1 cm² and a thickness of a few millimeters.

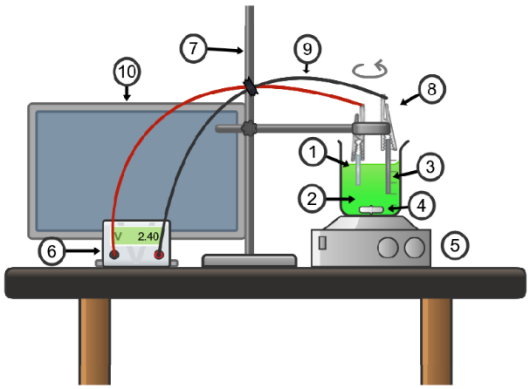

Fig. 3. *Electrodeposition system. 1. Nickel electrode. 2. Synthesis electrolyte. 3. Stainless steel electrode. 4. Magnetic stir bar. 5. Magnetic stirrer and heater. 6. Voltage or current source. 7. Vertical support. 8. Clamps. 9. Cables. 10. Computer with software for acquiring data from the Arduino.*

2.2 Data acquisition

The power supply for electrodeposition was precisely regulated with a Wuzhi WZ5005 DC-DC voltage regulator, which has a supply voltage range of (6-55) VDC and output parameters of (0-50) VDC and (0-5) A, with delivery accuracy of 0.01V and 0.001A for voltage and current respectively.

Although the voltage regulator has a display, a voltage divider circuit connected in parallel with the positive and negative terminals was implemented, which allows us to store the data.

On the other hand, because current readings were necessary, a Hall effect sensor was used. This was connected in series with the voltage regulator's power supply circuit to the electrodeposition system.

Finally, an Arduino Mega board was used for data acquisition and programming of sampling times. The sensors and reading circuits were connected to the board via analog ports, which have a 10-bit ADC module for (0-5) VDC signals. The data was stored on a microSD card using a datalogger that communicated with the Arduino via SPI protocol, creating a .TXT file for statistical analysis.

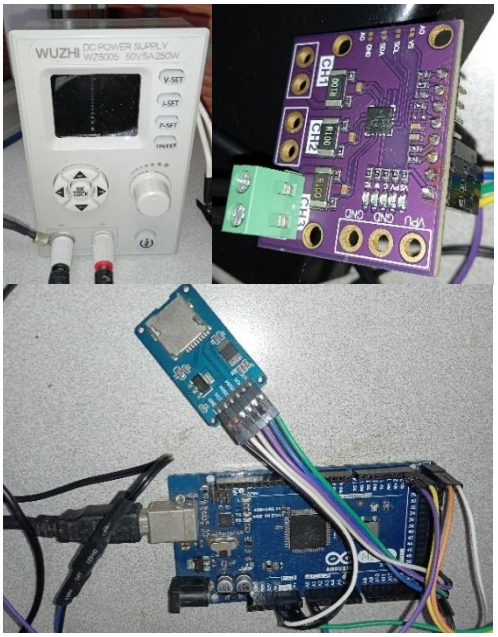

Fig. 4. *Top left: voltage regulator. Top right: hall effect sensor. Bottom: "datalogger" and Arduino Mega.*

2.3 Synthesis

The synthesis experiments were carried out with Ni(NO_3)_2*6H_2 O (0.05mol/l) and Na_2 S_2 O_3*5H_2 O (0.1mol/l) with stirring for 10min, as shown in Figure 5 and which correspond to 24 syntheses each with one replicate that are presented in Table 5, in which treatment I is identified which corresponds to cycles of 1, 3, 4 and 7 for the voltages of 0.54-0.84-1.14-1.24 V which correspond to series 1, then for the voltages of 0.7-0.92-1.17-1.63 V which correspond to series 2 and then for the voltages of 1.37-1.68-1.94-2.4 V which correspond to series 3; and also identifies treatment II which corresponds to series 1, 2 and 3 with an additional 4-minute cycle at the maximum voltage of each synthesis.

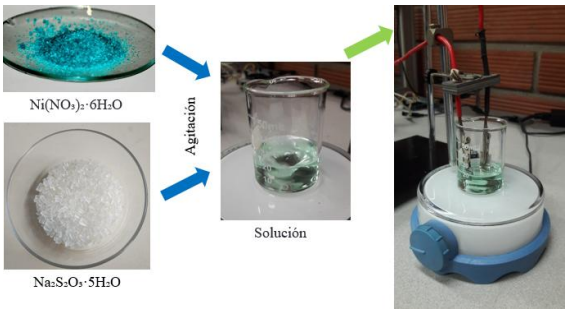

Fig. 5. *Synthesis scheme I.*

Table 5: *Set of experiments that were carried out for the synthesis, in this are the sample label, the voltage supplied per minute and the number of cycles; first is treatment I and then treatment II which corresponds to the additional cycle.*

Treatment I		
Sample	Voltage (V)	Cycles
1	0.54 – 0.84 – 1.14 – 1.24	1
2		3
3		4
4		7
5	0.7 – 0.92 – 1.17 – 1.63	1
6		3
7		4
8		7
9	1.37 – 1.68 – 1.94 – 2.4	1
10		3
11		4
12		7

Treatment II			
Sample	Voltage (V)	Cycles	Additional
13	0.54 – 0.84 – 1.14 – 1.24	1	4 minutos a 1.24 V
14		3	
15		4	
16		7	
17	0.7 – 0.92 – 1.17 – 1.63	1	4 minutos a 1.63 V
18		3	
19		4	
20		7	
21	1.37 – 1.68 – 1.94 – 2.4	1	4 minutos a 2.4 V
22		3	
23		4	
24		7	

This synthesis route was determined after an analysis of different options [17], [18], [19], [20], [21].

3. RESULTS AND ANALYSIS

3.1 Synthesis

In the synthesis, two (2) treatments were developed, each with its own particularities, which will be developed and explained in a differentiated manner in Treatment I and Treatment II respectively.

3.1.1 Treatment I

In Treatment I, three series of experiments were performed, as follows:

Series 1: Samples 1 to 4.
Series 2: Samples 5 to 8.
Series 3: Samples 9 to 12.

Series 1 uses a voltage range of 0.7V. In sample 1 (Figure 6), as in its replicate, it can be observed that the current at the beginning of the synthesis shows an increase, that is, when the voltage is 0.54V, which subsequently decreases gradually in that first cycle. Subsequently, for the second voltage level, there is again an increase in the current, although this time almost to the same value as the initial current. In the third voltage level, the current shows a greater increase and then a decay, and finally, in the fourth voltage level where we are at 1.24V, the highest current peak of the entire synthesis is observed. This may be due to the increase in potential and the passivation of the current in each of the levels, and it may be due to the fact that the system is incorporating layers of material on the electrode, and this decreases the current as time passes.

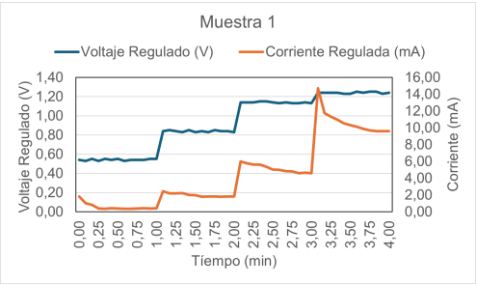

Fig. 6. *Sample 1, with one cycle, for four voltage levels.*

In Sample 2 (Figure 7), as in its replicate, the current exhibits a similar behavior to Samples 1 and 1* during the first cycle. However, during the second cycle, the current at the first voltage level is almost zero. This pattern is repeated for the third cycle and is much more pronounced at the second level, where it almost disappears, potentially indicating electrode passivation. Additionally, the current peaks at voltage level four decrease in intensity during all three cycles, suggesting system stability.

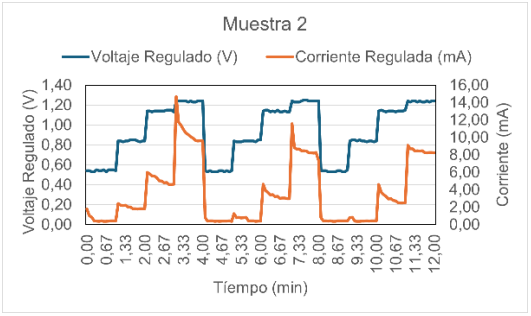

Fig. 7. *Sample 2, with three cycles, for four voltage levels.*

In sample 3 (Figure 8) as in its replica, for the fourth cycle it is observed that the current in the first voltage level is practically non-existent as well as for the second voltage level, even so for the third and fourth voltage level in the fourth cycle a very stable system is evident, which may be indicating a passivation of the electrode.

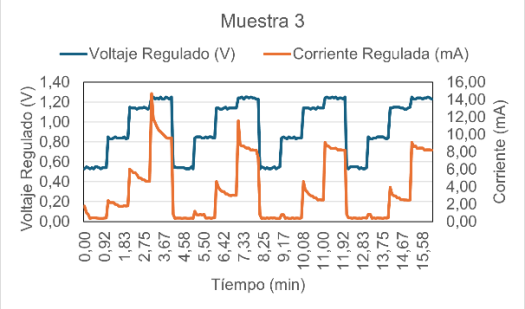

Fig. 8. *Sample 3, with four cycles, for four voltage levels.*

In sample 4 (Figure 9) as in its replica, for the fifth, sixth and seventh cycles it is observed that the current in the first two voltage levels is almost zero, even so for the third and fourth voltage level, in the fifth, sixth and seventh cycles a very stable system is evident, with a little increase for the current peak in the seventh cycle, this behavior is present from the third cycle.

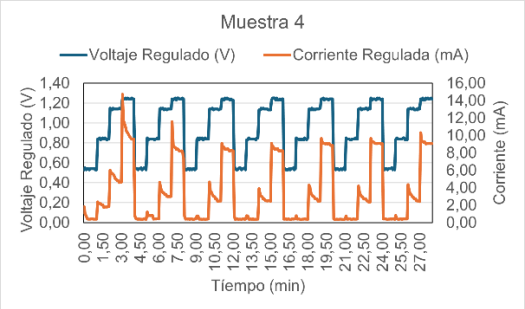

Fig. 9. *Sample 4, with seven cycles, for four voltage levels.*

The peak currents in samples 1, 2, 3, and 4 ranged from 14.71 mA to 8.63 mA.

In series 2, the voltage range was 0.93 V. The current exhibited similar behavior to the previous samples, with peak currents of 20.02 mA and 11.09 mA.

In series 3, the voltage range was 1.03 V. The current exhibited similar behavior to the previous samples, with peak currents of 28.22 mA and 16.59 mA.

It should be added that the voltage remained stable in all experiments and for all cycles.

3.1.2 Treatment II

In Treatment II, three series of experiments were performed, as follows:

Series 1: samples 13 to 16.
Series 2: samples 17 to 20.
Series 3: samples 21 to 24.

In samples 13, 14, 15, and 16 (Figure 11) and their respective replicates, samples 13*, 14*, 15*, and 16*, the voltage remained stable in all experiments and for all cycles. Regarding the current, it exhibited a similar behavior to the previous syntheses, with the difference that in the last cycle, the current remained stable with a difference of 1 mA for all samples.

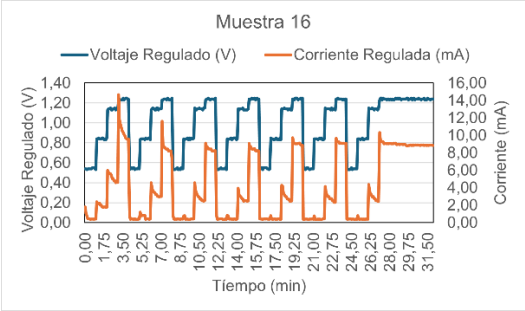

Fig. 10. *Sample 16, with eight cycles, for four voltage levels.*

In samples 17, 18, 19, and 20 (Figure 11) and their respective replicates, samples 17*, 18*, 19*, and 20*, the current exhibited a similar behavior to the previous syntheses, with the difference being a stable current in the last cycle with a difference of 1.95 mA for all samples. This same behavior was observed in samples 21, 22, 23, and 24 (Figure 13) and their respective replicates, samples 21*, 22*, 23*, and 24*, with the difference being a stable current in the last cycle with a difference of 2.83 mA for all samples.

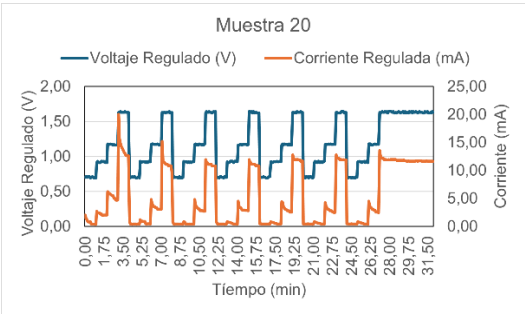

Fig. 11. *Sample 20, with eight cycles, for four voltage levels.*

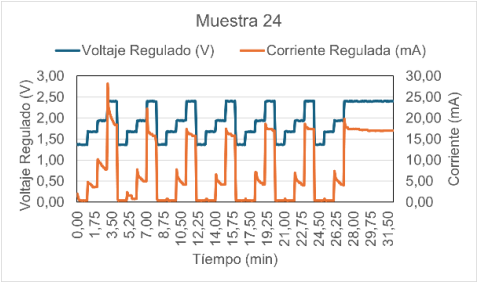

Fig. 12. *Sample 24, with eight cycles, for four voltage levels.*

Each sample was weighed before and after electrodeposition, and its values were recorded in the following table:

Sample	Initial Mass (g)	Final Mass (g)	Gain (g)
1	1,18258	1,18302	0,00044
1*	0,77618	0,77664	0,00046
2	0,86377	0,86492	0,00115
2*	0,97453	0,97557	0,00104
3	1,05432	1,05582	0,00150
3*	0,82215	0,82364	0,00149
4	0,94108	0,94358	0,00250
4*	1,12044	1,12302	0,00258
5	0,88763	0,88908	0,00145
5*	0,99231	0,99368	0,00137
6	0,79546	0,79748	0,00202
6*	1,08322	1,08522	0,00200
7	0,91457	0,91692	0,00235
7*	0,85690	0,85911	0,00221
8	1,15438	1,15788	0,00350
8*	0,83312	0,83657	0,00345
9	0,96745	0,96795	0,00050
9*	1,01239	1,01292	0,00053
10	0,78923	0,79063	0,00140
10*	0,87456	0,87594	0,00138
11	1,10231	1,10411	0,00180
11*	0,93412	0,93591	0,00179
12	0,84102	0,84416	0,00314
12*	0,98564	0,98887	0,00323
13	1,06744	1,06925	0,00181
13*	0,81235	0,81414	0,00179
14	0,89945	0,90197	0,00252
14*	1,14238	1,14492	0,00254
15	0,77894	0,78182	0,00288
15*	0,95671	0,95964	0,00293
16	1,03452	1,03902	0,00450
16*	0,86542	0,86995	0,00453
17	0,92218	0,92295	0,00077
17*	1,09874	1,09954	0,00080
18	0,80321	0,80534	0,00213
18*	0,88124	0,88324	0,00200
19	1,17125	1,17400	0,00275
19*	0,94563	0,94834	0,00271
20	1,02347	1,02812	0,00465
20*	0,85231	0,85702	0,00471
21	0,79122	0,79405	0,00283
21*	1,13456	1,13715	0,00259
22	0,90874	0,91253	0,00379
22*	0,97654	0,98023	0,00369
23	1,04562	1,05003	0,00441
23*	0,82945	0,83388	0,00443
24	0,89321	0,89958	0,00637
24*	1,11235	1,11892	0,00657

The analysis of the data allowed us to determine the mass gain and then, by analyzing the treatments individually by cycles, graph a comparison of the growth of treatment I against treatment II (Figure 13). In this way, we found that there is no significant difference between the treatments and that the additional cycle in treatment II adds mass regularly to the electrodes.

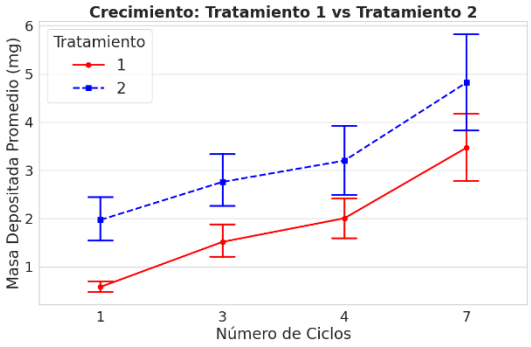

Fig. 13. *Comparison of average deposited mass for each treatment.*

4. RECOGNITION

Thanks to the University of Antioquia, the TESLA Research Group, and Professor Claudia Patricia Parra Medina for all their contributions.

5. CONCLUSIONS

The electrode coating synthesis protocol, via electrodeposition synthesis, is controllable for voltage and number of cycles.

These results suggest that electrodeposition is a promising technique for fabricating nickel sulfide-based electrodes or electronic devices.

Electrodeposition synthesis for multiple cycles shows a decay of current over time, indicating that the system is entering a passive state in which the electrodeposition rate decreases.

REFERENCES

[1] K. Richardson et al., “Earth beyond six of nine planetary boundaries”, *Science Advances*, vol. 9, núm. 37, sep. 2023, doi:10.1126/sciadv.adh2458.

[2] B. Sakschewski et al., Planetary Health Check 2025 A Scientific Assessment of the State of the Planet. 2025. doi:10.48485/pik.2025.017.

[3] A. O. Oni, K. Anaya, T. Giwa, G. Di Lullo, y A. Kumar, “Comparative assessment of blue hydrogen from steam methane reforming, autothermal reforming, and natural gas decomposition technologies for natural gas-producing regions”, *Energy Convers. Manag.*, vol. 254, p. 115245, 2022, doi:10.1016/j.enconman.2022.115245.

[4] N. M Santhosh, S. Gupta, V. Shvalya, M. Košiček, J. Zavašnik, y U. Cvelbar, “Advancing Oxygen Evolution Catalysis with Dual-Phase Nickel Sulfide Nanostructures”, *Energy & Fuels*, vol. 39, núm. 2, pp. 1375–

1383, ene. 2025, doi:10.1021/acs.energyfuels.4c05182.

[5] Y. Chen et al., "Nickel sulfide-based electrocatalysts for overall water splitting", *International Journal of Hydrogen Energy*, vol. 48, núm. 72, pp. 27992–28017, ago. 2023, doi:10.1016/j.ijhydene.2023.04.023.

[6] R.-C. Li et al., "One-step controlled electrodeposition nickel sulfides heterointerfaces favoring the desorption of hydroxyl groups for efficient hydrogen generation", *Rare Metals*, vol. 43, núm. 9, pp. 4377–4386, 2024, doi:10.1007/s12598-024-02806-6.

[7] Z. Wan et al., "Interface engineering of NiS/NiCo2S4 heterostructure with charge redistribution for boosting overall water splitting", *J. Colloid Interface Sci.*, vol. 653, pp. 795–806, 2024, doi:10.1016/j.jcis.2023.09.117.

[8] S. Haghverdi Khamene, N. van Dalen, M. Creatore, y M. N. Tsampas, "Structural and Electrochemical Evolution of Nickel Sulfides During Alkaline Hydrogen Evolution Reaction", *ChemSusChem*, dic. 2025, doi:10.1002/cssc.202501880.

[9] C. Lyu et al., "Electrodeposition and Optimisation of Amorphous Ni x S y Catalyst for Hydrogen Evolution Reaction in Alkaline Environment", *Chemistry – A European Journal*, vol. 30, núm. 66, nov. 2024, doi:10.1002/chem.202403030.

[10] P. Wang et al., "Interface Engineering of Ni_xS_y@MnOxHy Nanorods to Efficiently Enhance Overall-Water-Splitting Activity and Stability", *Nano-Micro Letters*, vol. 14, núm. 1, p. 120, dic. 2022, doi:10.1007/s40820-022-00860-2.

[11] W. Tan y H. He, "One-step electrodeposition of W, Mo-Ni 3 S 2 /NF catalyst: an efficient hydrogen evolution electrode for alkaline media", *RSC Advances*, vol. 15, núm. 47, pp. 39355–39367, 2025, doi:10.1039/D5RA07318A.

[12] R. Li, P. Kuang, S. Wageh, A. A. Al-Ghamdi, H. Tang, y J. Yu, "Potential-dependent reconstruction of Ni-based cuboid arrays for highly efficient hydrogen evolution coupled with electro-oxidation of organic compound", *Chemical Engineering Journal*, vol. 453, p. 139797, 2023, doi:10.1016/j.cej.2022.139797.

[13] I. A. Poimenidis, M. Lykaki, N. Papakosta, P. A. Loukakos, N. Kallithrakas Kontos, y M. Konsolakis, "One-step electrodeposition of NiS heterostructures on nickel foam electrodes for hydrogen evolution reaction: On the impact of thiourea content", *Results Chem.*, vol. 6, p. 101216, 2023, doi10.1016/j.rechem.2023.101216.

[14] D. Montgomery y C. St, Design and Analysis of Experiments, 9th Edition. 2022.

[15] D. McKenzie, "Designing and analysing powerful experiments: practical tips for applied researchers", *Fiscal Studies*, vol. 46, núm. 3, pp. 305–322, sep. 2025, doi:10.1111/1475-5890.70003.

[16] C. Miao et al., "Facile Electrodeposition of Amorphous Nickel/Nickel Sulfide Composite Films for High-Efficiency Hydrogen Evolution Reaction", *ACS Appl. Energy Mater.*, vol. 4, núm. 1, pp. 927–933, ene. 2021, doi:10.1021/acsaem.0c02863.

[17] B. Qiao et al., "Ni_xS_y/NF composites assembled by sulfidation of nickel foam (NF) for highly effective capture of iodine", *Chemical Engineering Journal*, vol. 479, p. 147864, 2024, doi:10.1016/j.cej.2023.147864.

[18] S. Esmailzadeh, T. Shahrabi, Gh. Barati Darband, y Y. Yaghoubinezhad, "Pulse electrodeposition of nickel selenide nanostructure as a binder-free and high-efficient catalyst for both electrocatalytic hydrogen and oxygen evolution reactions in alkaline solution", *Electrochim. Acta*, vol. 334, p. 135549, 2020, doi:10.1016/j.electacta.2019.135549.

[19] B. Zhong, S. Wan, P. Kuang, B. Cheng, L. Yu, y J. Yu, "Crystalline/amorphous Ni/Ni_xS_y supported on hierarchical porous nickel foam for high-current-density hydrogen evolution", *Appl. Catal. B*, vol. 340, p. 123195, ene. 2024, doi:10.1016/j.apcatb.2023.123195.

[20] P. Kotei, N. Boadi, S. Saah, y M. Mensah, "Synthesis of Nickel Sulfide Thin Films and Nanocrystals from the Nickel Ethyl Xanthate Complex", *Advances in Materials Science and Engineering*, vol. 2022, pp. 1–10, jul. 2022 doi:10.1155/2022/6587934.

[21] Y.-K. Hsu, A. Mondal, Y.-Z. Su, Z. Sofer, K. Shanmugam Anuratha, y J.-Y. Lin, "Highly hydrophilic electrodeposited NiS/Ni3S2 interlaced nanosheets with surface-enriched Ni3+ sites as binder-free flexible cathodes for high-rate hybrid supercapacitors", *Appl. Surf. Sci.*, vol. 579, p. 151923, 2022, doi:10.1016/j.apsusc.2021.151923.